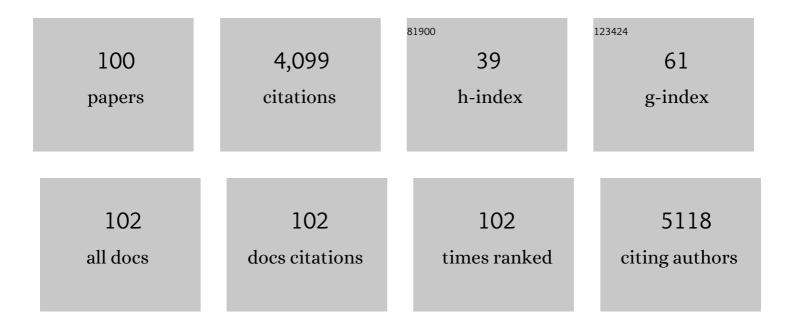


## List of Publications by Year in descending order

Source: https://exaly.com/author-pdf/3495110/publications.pdf Version: 2024-02-01



LIE CAO

#	Article	IF	CITATIONS
1	Supramolecular "Trojan Horse―for Nuclear Delivery of Dual Anticancer Drugs. Journal of the American Chemical Society, 2017, 139, 2876-2879.	13.7	253
2	Enzymeâ€Instructed Selfâ€Assembly (EISA) and Hydrogelation of Peptides. Advanced Materials, 2020, 32, e1805798.	21.0	193
3	Enzyme Promotes the Hydrogelation from a Hydrophobic Small Molecule. Journal of the American Chemical Society, 2009, 131, 11286-11287.	13.7	170
4	Utilization of steel slag as aggregate in asphalt mixtures for microwave deicing. Journal of Cleaner Production, 2017, 152, 429-442.	9.3	147
5	Nitric oxide releasing hydrogel enhances the therapeutic efficacy of mesenchymal stem cells for myocardial infarction. Biomaterials, 2015, 60, 130-140.	11.4	132
6	Recognition, location, measurement, and 3D reconstruction of concealed cracks using convolutional neural networks. Construction and Building Materials, 2017, 146, 775-787.	7.2	125
7	Liposome-based glioma targeted drug delivery enabled by stable peptide ligands. Journal of Controlled Release, 2015, 218, 13-21.	9.9	113
8	Ultrasensitive and specific fluorescence detection of a cancer biomarker <i>via</i> nanomolar binding to a guanidinium-modified calixarene. Chemical Science, 2018, 9, 2087-2091.	7.4	113
9	Incorporation of supramolecular hydrogels into agarose hydrogels—a potential drug delivery carrier. Journal of Materials Chemistry, 2009, 19, 7892.	6.7	98
10	Microwave deicing for asphalt mixture containing steel wool fibers. Journal of Cleaner Production, 2019, 206, 1110-1122.	9.3	97
11	IGF-1 C Domain–Modified Hydrogel Enhances Cell Therapy for AKI. Journal of the American Society of Nephrology: JASN, 2016, 27, 2357-2369.	6.1	96
12	Characteristics of dissolved organic matter (DOM) and relationship with dissolved mercury in Xiaoqing River-Laizhou Bay estuary, Bohai Sea, China. Environmental Pollution, 2017, 223, 19-30.	7.5	90
13	Recognition of asphalt pavement crack length using deep convolutional neural networks. Road Materials and Pavement Design, 2018, 19, 1334-1349.	4.0	89
14	Design of Y-shaped targeting material for liposome-based multifunctional glioblastoma-targeted drug delivery. Journal of Controlled Release, 2017, 255, 132-141.	9.9	74
15	Enhanced cycle performance of ultraflexible asymmetric supercapacitors based on a hierarchical MnO <sub>2</sub> @NiMoO <sub>4</sub> core–shell nanostructure and porous carbon. Journal of Materials Chemistry A, 2016, 4, 18181-18187.	10.3	73
16	Advances of deep learning applications in ground-penetrating radar: A survey. Construction and Building Materials, 2020, 258, 120371.	7.2	73
17	Supramolecular Nanofibers with Superior Bioactivity to Insulin-Like Growth Factor-I. Nano Letters, 2019, 19, 1560-1569.	9.1	71
18	Dispersion of carbon fibers in cement-based composites with different mixing methods. Construction and Building Materials, 2017, 134, 220-227.	7.2	69

#	Article	IF	CITATIONS
19	Effect of microplastics on ecosystem functioning: Microbial nitrogen removal mediated by benthic invertebrates. Science of the Total Environment, 2021, 754, 142133.	8.0	68
20	Innovative method for recognizing subgrade defects based on a convolutional neural network. Construction and Building Materials, 2018, 169, 69-82.	7.2	67
21	Pavement-distress detection using ground-penetrating radar and network in networks. Construction and Building Materials, 2020, 233, 117352.	7.2	64
22	Folic Acid Derived Hydrogel Enhances the Survival and Promotes Therapeutic Efficacy of iPS Cells for Acute Myocardial Infarction. ACS Applied Materials & Interfaces, 2018, 10, 24459-24468.	8.0	63
23	Convolutional Neural Network for Asphalt Pavement Surface Texture Analysis. Computer-Aided Civil and Infrastructure Engineering, 2018, 33, 1056-1072.	9.8	62
24	Self-healing behavior of asphalt system based on molecular dynamics simulation. Construction and Building Materials, 2020, 254, 119225.	7.2	61
25	Stabilized Heptapeptide A7R for Enhanced Multifunctional Liposome-Based Tumor-Targeted Drug Delivery. ACS Applied Materials & Interfaces, 2016, 8, 13232-13241.	8.0	58
26	Autonomous pavement distress detection using ground penetrating radar and region-based deep learning. Measurement: Journal of the International Measurement Confederation, 2020, 164, 108077.	5.0	57
27	Magnetic porous carbon nanocomposites derived from metal-organic frameworks as a sensing platform for DNA fluorescent detection. Analytica Chimica Acta, 2016, 940, 136-142.	5.4	54
28	RGD-modified lipid disks as drug carriers for tumor targeted drug delivery. Nanoscale, 2016, 8, 7209-7216.	5.6	54
29	A stapled peptide antagonist of MDM2 carried by polymeric micelles sensitizes glioblastoma to temozolomide treatment through p53 activation. Journal of Controlled Release, 2015, 218, 29-35.	9.9	51
30	Dual enzymes regulate the molecular self-assembly of tetra-peptide derivatives. Soft Matter, 2011, 7, 10443.	2.7	50
31	Recent Progress in the Vinylic Polymerization and Copolymerization of Norbornene Catalyzed by Transition Metal Catalysts. Polymer Reviews, 2009, 49, 249-287.	10.9	49
32	Pavement defect detection with fully convolutional network and an uncertainty framework. Computer-Aided Civil and Infrastructure Engineering, 2020, 35, 832-849.	9.8	48
33	Lanthanide/nucleotide coordination polymers: an excellent host platform for encapsulating enzymes and fluorescent nanoparticles to enhance ratiometric sensing. Journal of Materials Chemistry B, 2017, 5, 7692-7700.	5.8	48
34	A Mixed Component Supramolecular Hydrogel to Improve Mice Cardiac Function and Alleviate Ventricular Remodeling after Acute Myocardial Infarction. Advanced Functional Materials, 2017, 27, 1701798.	14.9	47
35	Characterization of carbon fiber distribution in cement-based composites by Computed Tomography. Construction and Building Materials, 2018, 177, 134-147.	7.2	47
36	Utilization of magnetite tailings as aggregates in asphalt mixtures. Construction and Building Materials, 2016, 114, 392-399.	7.2	44

#	Article	IF	CITATIONS
37	Quantitative evaluation of carbon fiber dispersion in cement based composites. Construction and Building Materials, 2014, 68, 26-30.	7.2	42
38	Evaluating the cycling comfort on urban roads based on cyclists' perception of vibration. Journal of Cleaner Production, 2018, 192, 531-541.	9.3	42
39	Self-assembly of semiflexible block copolymers: 2D numerical implementation of self-consistent field theory. Soft Matter, 2011, 7, 5208.	2.7	40
40	Study on the optimum rice husk ash content added in asphalt binder and its modification with bio-oil. Construction and Building Materials, 2017, 147, 776-789.	7.2	40
41	One-step synthesis of V <sub>2</sub> O <sub>5</sub> /Ni <sub>3</sub> S <sub>2</sub> nanoflakes for high electrochemical performance. Journal of Materials Chemistry A, 2017, 5, 23543-23549.	10.3	39
42	Early events in rabies virus infection—Attachment, entry, and intracellular trafficking. Virus Research, 2019, 263, 217-225.	2.2	38
43	A stabilized peptide ligand for multifunctional glioma targeted drug delivery. Journal of Controlled Release, 2016, 243, 86-98.	9.9	36
44	Self-assembled GFFYK peptide hydrogel enhances the therapeutic efficacy of mesenchymal stem cells in a mouse hindlimb ischemia model. Acta Biomaterialia, 2019, 85, 94-105.	8.3	35
45	Laboratory Investigation on Microwave Deicing Function of Micro Surfacing Asphalt Mixtures Reinforced by Carbon Fiber. Journal of Testing and Evaluation, 2014, 42, 498-507.	0.7	35
46	Differential calixarene receptors create patterns that discriminate glycosaminoglycans. Organic Chemistry Frontiers, 2018, 5, 2685-2691.	4.5	33
47	Hierarchical polypyrrole/Ni <sub>3</sub> S <sub>2</sub> @MoS <sub>2</sub> core–shell nanostructures on a nickel foam for high-performance supercapacitors. RSC Advances, 2016, 6, 68460-68467.	3.6	32
48	Kinetic and thermodynamic modeling of Portland cement hydration at low temperatures. Chemical Papers, 2017, 71, 741-751.	2.2	30
49	ZnO nanorod/nickel phthalocyanine hierarchical hetero-nanostructures with superior visible light photocatalytic properties assisted by H <sub>2</sub> O <sub>2</sub> . RSC Advances, 2015, 5, 87233-87240.	3.6	25
50	Dual-emissive polystyrene@zeolitic imidazolate framework-8 composite for ratiometric detection of singlet oxygen. Journal of Materials Chemistry B, 2017, 5, 9175-9182.	5.8	25
51	PNOC Expressed by B Cells in Cholangiocarcinoma Was Survival Related and LAIR2 Could Be a T Cell Exhaustion Biomarker in Tumor Microenvironment: Characterization of Immune Microenvironment Combining Single-Cell and Bulk Sequencing Technology. Frontiers in Immunology, 2021, 12, 647209.	4.8	25
52	Genome-wide DNA methylation analysis in permanent atrial fibrillation. Molecular Medicine Reports, 2017, 16, 5505-5514.	2.4	23
53	Three-dimensional texture measurement using deep learning and multi-view pavement images. Measurement: Journal of the International Measurement Confederation, 2021, 172, 108828.	5.0	23
54	Monitoring and optimizing the surface roughness of high friction exposed aggregate cement concrete in exposure process. Construction and Building Materials, 2020, 230, 117005.	7.2	22

#	Article	IF	CITATIONS
55	Social defeat stress before pregnancy induces depressive-like behaviours and cognitive deficits in adult male offspring: correlation with neurobiological changes. BMC Neuroscience, 2018, 19, 61.	1.9	21
56	D-SP5 Peptide-Modified Highly Branched Polyethylenimine for Gene Therapy of Gastric Adenocarcinoma. Bioconjugate Chemistry, 2015, 26, 1494-1503.	3.6	20
57	A facile one-pot hydrothermal synthesis of Co <sub>9</sub> S <sub>8</sub> /Ni <sub>3</sub> S <sub>2</sub> nanoflakes for supercapacitor application. RSC Advances, 2016, 6, 54142-54148.	3.6	19
58	Cycling comfort on asphalt pavement: Influence of the pavement-tyre interface on vibration. Journal of Cleaner Production, 2019, 223, 323-341.	9.3	19
59	A novel method for multi-scale carbon fiber distribution characterization in cement-based composites. Construction and Building Materials, 2019, 218, 40-52.	7.2	18
60	Autonomous microscopic bunch inspection using region-based deep learning for evaluating graphite powder dispersion. Construction and Building Materials, 2018, 173, 525-539.	7.2	17
61	Preorganization Increases the Self-Assembling Ability and Antitumor Efficacy of Peptide Nanomedicine. ACS Applied Materials & Interfaces, 2020, 12, 22492-22498.	8.0	17
62	Improvement of mechanical properties and chloride ion penetration resistance of cement pastes with the addition of pre-dispersed silica fume. Construction and Building Materials, 2018, 182, 483-492.	7.2	16
63	Wearable Thermoelectric Cooler Based on a Two-Layer Hydrogel/Nickel Foam Heatsink with Two-Axis Flexibility. ACS Applied Materials & Interfaces, 2022, 14, 15317-15323.	8.0	16
64	Ratiometric detection of hydroxy radicals based on functionalized europium(III) coordination polymers. Mikrochimica Acta, 2018, 185, 9.	5.0	15
65	A <scp>D</scp> â€Peptide Ligand of Nicotine Acetylcholine Receptors for Brainâ€Targeted Drug Delivery. Angewandte Chemie, 2015, 127, 3066-3070.	2.0	14
66	Reinforcement of power factor in N-type multiphase thin film of Si1â´'xâ´'yGexSny by mitigating the opposing behavior of Seebeck coefficient and electrical conductivity. Applied Physics Letters, 2021, 119, .	3.3	14
67	A new method for CF morphology distribution evaluation and CFRC property prediction using cascade deep learning. Construction and Building Materials, 2019, 222, 829-838.	7.2	13
68	Enzyme-instructed self-assembly (EISA) assists the self-assembly and hydrogelation of hydrophobic peptides. Journal of Materials Chemistry B, 2022, 10, 3242-3247.	5.8	13
69	Surprisingly fast assembly of the MOF film for synergetic antibacterial phototherapeutics. Green Chemistry, 2022, 24, 5930-5940.	9.0	13
70	Glioma-Targeted Drug Delivery Enabled by a Multifunctional Peptide. Bioconjugate Chemistry, 2017, 28, 775-781.	3.6	12
71	Innovation for evaluating aggregate angularity based upon 3D convolutional neural network. Construction and Building Materials, 2017, 155, 919-929.	7.2	12
72	Portland Cement Hydration Behavior at Low Temperatures: Views from Calculation and Experimental Study. Advances in Materials Science and Engineering, 2017, 2017, 1-9.	1.8	12

#	Article	IF	CITATIONS
73	2D Salphen-based heteropore covalent organic frameworks for highly efficient electrocatalytic water oxidation. Chemical Communications, 2021, 57, 13162-13165.	4.1	12
74	Reduction-triggered formation of EFK8 molecular hydrogel for 3D cell culture. RSC Advances, 2014, 4, 30168.	3.6	11
75	A CoOOH nanoflake-based light scattering probe for the simple and selective detection of uric acid in human serum. Analytical Methods, 2018, 10, 4951-4957.	2.7	11
76	Combination of pixel-wise and region-based deep learning for pavement inspection and segmentation. International Journal of Pavement Engineering, 2022, 23, 3011-3023.	4.4	11
77	Iron phthalocyanine nanorods for ethanol sensoring. Micro and Nano Letters, 2016, 11, 348-350.	1.3	10
78	Lipase-catalyzed synthesis and characterization of myristoyl maltose ester. European Food Research and Technology, 2011, 233, 253-258.	3.3	8
79	Entry of Challenge Virus Standard (CVS) -11 into N2a cells via a clathrin-mediated, cholesterol-, dynamin-, pH-dependent endocytic pathway. Virology Journal, 2019, 16, 80.	3.4	8
80	Supramolecular protein glue to boost enzyme activity. Science China Materials, 2019, 62, 1341-1349.	6.3	8
81	Study on the reaction performance of Ceâ€doped <scp> NiFe <sub>2</sub> O <sub>4</sub> </scp> oxygen carriers in the process of chemical looping hydrogen production. International Journal of Energy Research, 2022, 46, 2810-2825.	4.5	8
82	Controlling the width of nanosheets by peptide length in peptoid–peptide biohybrid hydrogels. RSC Advances, 2016, 6, 67025-67028.	3.6	7
83	Prediction of Electrical Conductivity of Fiber-Reinforced Cement-Based Composites by Deep Neural Networks. Materials, 2019, 12, 3868.	2.9	7
84	Tandem molecular self-assembly for selective lung cancer therapy with an increase in efficiency by two orders of magnitude. Nanoscale, 2021, 13, 10891-10897.	5.6	7
85	Two-Incision Totally Thoracoscopic Approach for Mitral Valve Replacement. International Heart Journal, 2017, 58, 894-899.	1.0	6
86	Investigation on Simultaneous Removal of SO <sub>2</sub> and NO over a Cu–Fe/TiO <sub>2</sub> Catalyst Using Vaporized H <sub>2</sub> O <sub>2</sub> : An Analysis on SO <sub>2</sub> Effect. Industrial & Engineering Chemistry Research, 2021, 60, 13474-13484.	3.7	6
87	Impact of anger emotional stress before pregnancy on adult male offspring. Oncotarget, 2017, 8, 98837-98852.	1.8	6
88	Manipulating the Solubility of SnSe in SnTe by Br Doping for Improving the Thermoelectric Performance. ACS Applied Energy Materials, 2021, 4, 13027-13035.	5.1	5
89	Study on the redox performance of Cu and <scp> Ceâ€doped CoFe <sub>2</sub> O <sub>4</sub> </scp> as oxygen carriers for chemical looping hydrogen generation. International Journal of Energy Research, 2022, 46, 7424-7440.	4.5	5
90	Oxidation-absorption process for simultaneous removal of NOx and SO2 over Fe/Al2O3@SiO2 using vaporized H2O2. Chemosphere, 2022, 291, 133047.	8.2	4

#	Article	IF	CITATIONS
91	A SupraGel for efficient production of cell spheroids. Science China Materials, 2022, 65, 1655-1661.	6.3	4
92	An amelogenin-based peptide hydrogel promoted the odontogenic differentiation of human dental pulp cells. International Journal of Energy Production and Management, 2022, 9, .	3.7	4
93	Isolation of a halophilic bacterium, Bacillus sp. strain NY-6 for organic contaminants removal in saline wastewater on ship. Journal of Marine Science and Application, 2013, 12, 245-249.	1.7	3
94	On the Computation of Concept Stability Based on Maximal Non-Generator for Social Networking Services. Applied Sciences (Switzerland), 2020, 10, 8618.	2.5	3
95	Resident intruder paradigm-induced aggression relieves depressive-like behaviors in male rats subjected to chronic mild stress. Medical Science Monitor, 2014, 20, 945-952.	1.1	3
96	Supramolecular silk from a peptide hydrogel. Materials Chemistry Frontiers, 2017, 1, 911-915.	5.9	2
97	Skyline ( <i>λ</i> , <i>k</i> )-Cliques Identification From Fuzzy Attributed Social Networks. IEEE Transactions on Computational Social Systems, 2022, 9, 1075-1086.	4.4	2
98	Dynein- and kinesin- mediated intracellular transport on microtubules facilitates RABV infection. Veterinary Microbiology, 2021, 262, 109241.	1.9	2
99	Functions of Bacillus Subtilis BS7.29 in Wasterwater Treatment. , 2010, , .		0
100	Rücktitelbild: AD-Peptide Ligand of Nicotine Acetylcholine Receptors for Brain-Targeted Drug Delivery (Angew. Chem. 10/2015). Angewandte Chemie, 2015, 127, 3194-3194.	2.0	0

(Angew. Chem. 10/2015). Angewandte Chemie, 2015, 127, 3194-3194.